Waters™

Nota de aplicación

Reversed-Phase LC-MS Analysis of Low-Abundance Impurities in a GLP-1a Therapeutic Using a Charged Surface 230Å Superficially Porous Phenyl-Hexyl Column

Stephan M. Koza, Stephen J. Shiner, Matthew A. Lauber

Waters Corporation, United States

Published on July 15, 2026

Abstract

Reversed-phase LC methods (RPLC) along with high-resolution mass spectrometry detection (RPLC-HRMS) for the purity analysis of therapeutic GLP-1a tirzepatide are presented. These methods highlight the utility of the Waters BioResolve™ Peptide Phenyl-Hexyl+ RP Column with MaxPeak™ Premier Technology (SPP, 1.6 µm, 230 Å, 2.1 x 150 mm), along with a Xevo™ G3 QTof Mass Spectrometer equipped with an ESI source, for lipopeptide analysis using acetonitrile gradients with either formic acid (FA) or trifluoroacetic acid (TFA) as a mobile-phase modifier. To take full advantage of the selectivity differences between the phenyl-hexyl and C_{18} ligands in RPLC, this column uses sub-2 µm superficially porous particles (SPP) that have a relatively wide 230 Å average pore diameter, a positively charged particle surface, and are packed into MaxPeak Premier Column hardware that minimizes protein and peptide surface interactions. In addition to detailed LC-MS examinations of low abundance tirzepatide impurities, the performance of this column was also compared to that of an alternative 2.7 µm, 90 Å charged surface SPP column.

In summary, these hyphenated RPLC-MS methods provide detailed mass information for a wide array of low-abundance impurities encountered in a GLP-1a lipopeptide drug product. In addition, the separation of several synthesized impurity standards is presented. The separation gradients deployed in this study were broad ranged with acetonitrile gradients of 1%/min at a flow rate of 0.30 mL/min resulting in analysis times of 46 minutes or less; however, opportunities exist for bespoke optimization to either reduce analysis time or improve resolution.

Benefits

Noted performance characteristics of the Waters BioResolve Peptide Phenyl-Hexyl RP Column include:

- Detailed RP-HRMS evaluations of low-abundance impurities in the therapeutic GLP-1a tirzepatide using either FA or TFA modified acetonitrile (MeCN) gradients
- Improved separations in FA mobile phases versus a 2.7 µm, 90 Å charged surface SPP column
- Alternative selectivity in comparison to C_{18} RPLC separations
- Column designation L11 in accordance with the General Chapter on Chromatography USP <621>

Introduction

Tirzepatide is a glucagon-like peptide-1 analog (GLP-1a) with an average molecular weight of 4813.53 Da and a monoisotopic mass of 4810.52 Da. GLP-1a lipopeptide constructs possess a fatty acid side chain that can present additional analytical challenges when developing RPLC purity analyses. The fatty acid side chain dominates the RP retention for lipopeptides and tends to shroud more subtle changes in the RPLC retention due to variations of the peptide backbone resulting from the manufacturing process (***e.g.*** amino acid substitutions) or degradation (***e.g.*** oxidation and deamidation). Outcomes of this characteristic may include the use of shallow extended gradients that greatly increase analysis times, or the addition of complementary analysis methods such as HILIC, IEX, and LCMS.[1-4]

In this study, RP-HRMS methods for the characterization of low-abundance impurities in a commercial tirzepatide liquid drug product along with the analysis of several tirzepatide impurity standards are demonstrated. Separations were performed using a BioResolve Peptide Phenyl-Hexyl+ RP Column (2.1 x 150 mm) with MaxPeak Premier Technology packed with 230 Å pore diameter, and 1.6 µm silica SPPs. These particles have positively charged surfaces and have been bonded with a phenyl-hexyl ligand. These particle

modifications result in a column that can be used effectively with a FA mobile phase and provide selectivity differences in comparison to a C_{18} ligand.[1] A Xevo G3 QTof Mass Spectrometer with an ESI was deployed for mass analysis using MeCN gradients of 1%/min at a flow rate of 0.30 mL/min with either 0.1% (v/v) FA or 0.1% (v/v) TFA as a mobile phase modifier.

Experimental

Sample Description

Tirzepatide (Mounjaro® at 30 mg/mL) was analyzed past expiry and diluted to 3 mg/mL in water prior to analysis. Synthetic tirzepatide impurity standards were obtained from BioFargo™ Inc. and included: L-isoAsp^{9}, L-isoAsp^{15}, C-terminal deamidation, Ile12Nva (substitution), Gln^{24} deamidation, Gln^{19} deamidation, and D-Ser^{32} (racemized).

Method Conditions

LC Conditions

LC system:	ACQUITY UPLC™ LC Instrument with Binary Solvent Manager (BSM), Flow-Through Needle (FTN) Sample Manager, and ACQUITY Tunable UV (TUV) Detector (5 mm flow cell)
Columns:	Waters BioResolve Peptide Phenyl-Hexyl+ RP Column, MaxPeak Premier Technology, SPP, 1.6 µm, 230 Å, 2.1 x 150 mm (p/n: 186011727) Alternative Vendor Column: SPP, 2.7 µm, 90 Å, 2.1 x 150 mm
Column temperature:	60 °C
Sample temperature:	6 °C

Injection volume:	0.5 µL or as indicated
Mobile phases:	A: 0.10% (v/v) TFA or FA in 18 MΩ water B: 0.10% (v/v) TFA or FA in MeCN (LCMS grade)
Flow rate:	0.30 mL/min
Detector:	Waters TUV Detector, 215 nm at 20 Hz
Data management:	UNIFI™ and waters_connect™ Platform

Xevo G3 QTof Mass Spectrometer Parameters

Low mass:	400 *m/z*
High mass:	2800 *m/z*
Scan time:	0.250 seconds
Collision energy mode:	Off (6V)
Intelligent data capture threshold:	Custom (1)
Source temperature:	120 °C
Desolvation temperature:	300 °C
Cone gas:	50 L/h
Desolvation gas:	750 L/h
Capillary voltage:	3.00 kV

Sample cone voltage:	20 V
Data collection and analysis:	UNIFI and waters_connect Platform and using BayesSpray deconvolution

Formic Acid (0.10% v/v) Gradient Table

Time (min)	Flow Rate (mL/min)	A (%)	B (%)
0.00	0.300	80.0	20.0
1.00	0.300	80.0	20.0
36.00	0.300	45.0	55.0
38.00	0.300	5.0	95.0
39.00	0.300	5.0	95.0
40.00	0.300	80.0	20.0
46.00	0.300	80.0	20.0

TFA (0.10% v/v) Gradient Table

Time (min)	Flow Rate (mL/min)	A (%)	B (%)
0.00	0.300	90.0	10.0
1.00	0.300	80.0	20.0
34.00	0.300	47.0	53.0
35.00	0.300	5.0	95.0
36.00	0.300	5.0	95.0
37.00	0.300	90.0	10.0
43.00	0.300	90.0	10.0

Results and Discussion

Chromatographic overlays of tirzepatide drug product and a series of tirzepatide impurity standards are shown in Figure 1. Gradients of 1% MeCN/min with mobile phases using 0.10% (v/v) TFA or FA as a modifier were used. While there are comparable selectivities with respect to the main drug product peak for the majority of the impurity peaks, the C-terminally deamidated and the L-isoAsp[9] impurities demonstrated substantial selectivity differences. Of these, the L-isoAsp[9] which eluted well after the main peak with FA and prior to the main peak with TFA had the most significant shift. These changes in selectivity between TFA and FA modifiers along with previously reported selectivity alterations in RPLC selectivity based on the ligand used and temperature highlight some of the levers that can be used to optimize these separations while also noting the critical importance in controlling separation conditions for these methods.[1,5]

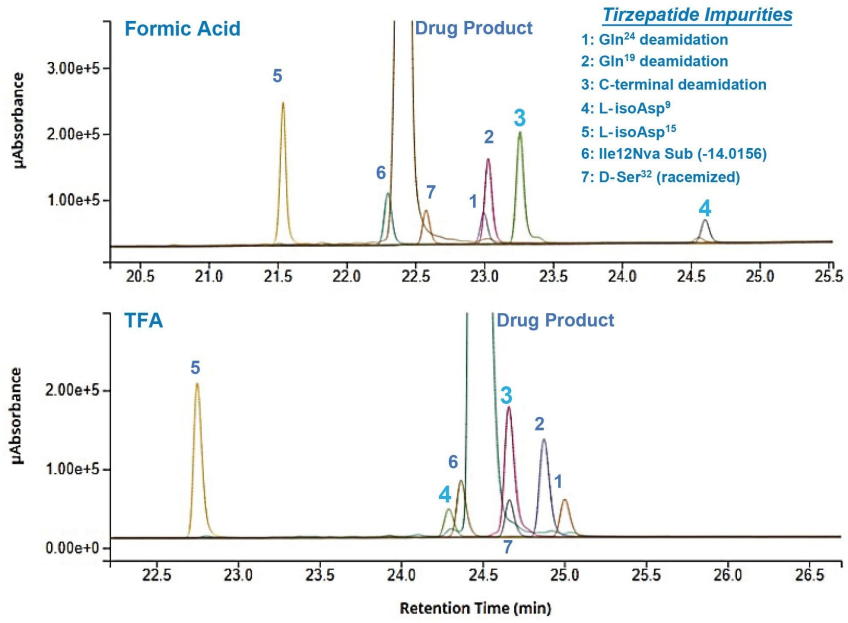

Figure 1. Mobile phase modifier selectivity differences of tirzepatide and several synthesized impurity standards observed with a Waters BioResolve Peptide phenyl-hexyl+ RP column (SPP, 1.6 µm, 2.1 x 150 mm) are shown. MeCN gradients (1% MeCN/min) with either TFA or FA modifiers (0.10% v/v) were evaluated at a flow rate of 0.30 mL/min. Significant changes in selectivity for impurities 3 and 4 are highlighted.

RP-HRMS results for tirzepatide drug product are presented in Figure 2 and Figure 3. Figure 2 shows both the

total intensity MS chromatograms (TIC) and the 215 nm UV absorbance (A215) traces for the separations using 0.1% FA in an MeCN gradient while Figure 3 presents those data for 0.1% TFA. Corresponding selected monoisotopic mass data for the labeled peaks are provided in Table 1 and Table 2. Predominant masses observed for both FA and TFA separations (< 6 PPM difference) are highlighted in a green italic font in Tables 1 and 2, while assigned peaks based on the impurity standard retention times (Figure 1) plus mass data are highlighted in a bold blue font, and unique predominant masses are in standard black font. The masses measured for the main tirzepatide peaks were consistent with the predicted values (+2.2 PPM error).

Wide arrays of low abundance variants were observed for both separations with the most abundant variant observed being Peak 5 (0.33% peak area) in the post-main peak zoom of the FA separation (Figure 2). The mass and retention time of this variant corresponds with the L-isoAsp^{9} impurity standard. As previously noted, L-isoAsp^{9} elutes prior to the main peak in the TFA separation and is tentatively identified as a co-eluting species under Peak 25 in the pre-main peak zoom (Figure 3). Most of the peaks observed were 1 to 2 orders lower in abundance than Peak 5 for both separations with many of those peaks being comprised of several variants based on the MS data.

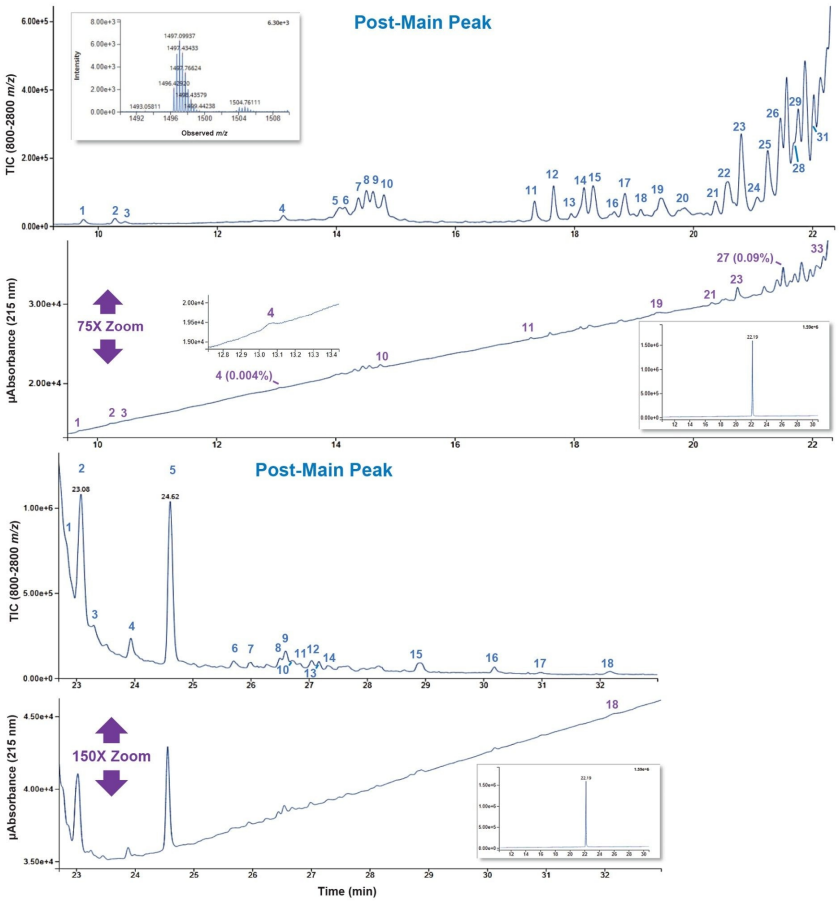

Figure 2. Impurities observed in a tirzepatide drug product are shown for a 1% MeCN/min gradient with FA modifier (0.10% v/v). The top two chromatograms depict the HRMS TIC and the A215 traces for impurities eluting prior to the main peak while impurities eluting after the main peak are shown in the bottom two chromatograms. Peak masses are provided in Table 1, and selected peak relative abundances are shown in parentheses. Full-scale A215 chromatograms and a zoomed view of pre-main peak 4 are shown as insets in the A215 chromatograms, and its raw MS data is an inset in the pre-main peak TIC.

Peak #	Pre-Peak	Post-Peak
1	*4067.069*	4753.504, 4723.491,4850.524
2	*4212.147*	**4811.528 (Gln^{19} & Gln^{24} deam.)**
3	*4357.218*	**4811.533 (C-term deam.)**, 3335.820
4	*4486.261*	4810.523
5	4125.077, *4270.166*, *4314.203*	**4810.534 (L-isoAsp^{9})**
6	4240.149, 4169.106	*4218.229*
7	*4298.146*	4822.530
8	*4153.070*, 4284.164	*4853.536*
9	*4342.172*	4838.525
10	*4197.101*	*9633.085*
11	*2990.59*	*4034.143*
12	*2991.575*	*4849.541*, 8688.416
13	*3098.620*	687.437*
14	*3046.655*	4809.506
15	*3046.654*, 2981.577	*4988.707*
16	3044.637	*4988.708*
17	*3115.672*, 3263.795	9512.010
18	*3089.650*	*4719.454*
19	*3825.121*, *3662.055*	
20	4824.511, 3435.826, 3952.083	
21	*4851.533*	
22	*4128.230*, *3275.798*	
23	*4792.527*, 4027.183, 4584.368	
24	4275.301	
25	*4376.348*, *4826.523*	
26	4829.516	
27	**4810.529 (L-isoAsp^{15})**	
28	*4562.410*	
29	4810.537, *4826.529*, 4647.471	
30	*4810.526, 4792.519, 4795.515*	
31	4842.526	
32	4867.566, 4814.520	
33	**4796.504 (Ile12Nva)**, 4897.564	
Main Peak	4810.535 (Predicted: 4810.525, 2.1 PPM error)	
Green: observed in FA and TFA, **Blue**: identified impurity standard, Black: only observed with FA		

Table 1. RP-HRMS Tirzepatide Monoisotopic Masses Observed (0.10% FA).

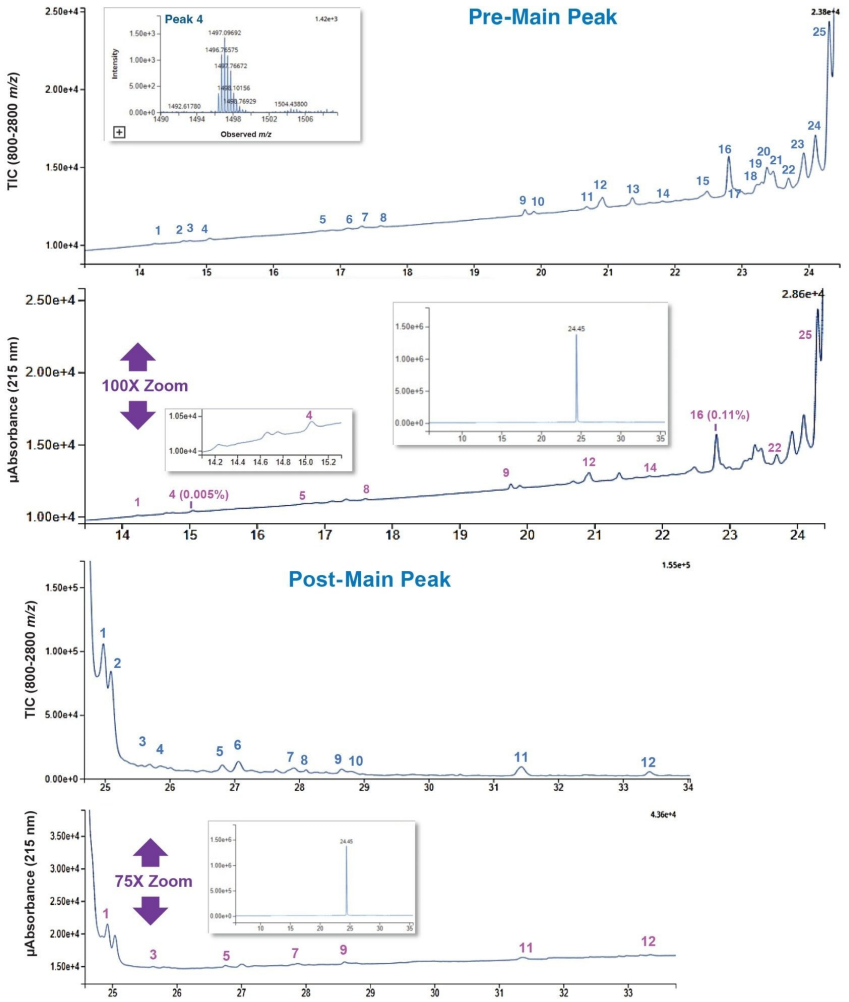

Figure 3: Impurities observed in a tirzepatide drug product are shown for a 1% MeCN/min gradient with TFA modifier (0.10% v/v). The top two chromatograms depict the HRMS TIC and the A215 traces for impurities eluting prior to the main peak while impurities eluting after the main peak are shown in the bottom two chromatograms. Peak masses are provided in Table 2, and selected peak relative abundances are shown in parentheses. Full-scale A215 chromatograms and a zoomed view of pre-main peak 4 are shown as insets in the A215 chromatograms, and its raw MS data is an inset in the pre-main peak TIC.

Peak #	Pre-Peak	Post-Peak
1	*4067.072*	**4811.525 (Gln[19] deam.)**
2	*4212.153*	4812.542
3	*4357.221*	4433.328, 4362.284
4	*4486.266*	*4792.534*, 6558.454
5	*4314.178, 4270.151*	*4218.243*
6	*4298.165*, 3059.615	*4853.551*, *4849.550*
7	*4153.078, 4342.176*	*4034.156*, *4719.464*
8	*4197.104*, 3114.687	*9632.159*
9	*2991.585*	3977.1, *9633.098*
10	*2990. 603*	7898.177, 3920.114
11	3061.637, *3098.633*	*4988.704*
12	*3046.661*	*4988.704*
13	*3275.806, 3115.682*	
14	*3089.662*	
15	*4851.534*, *4810.535*, 3436.805	
16	**4810.537 (L-isoAsp[15])**	
17	*4842.532*	
18	*3825.124, 3662.058*	
19	*4826.539*	
20	*4792.527*, *4128.237*	
21	*4826.528*	
22	*4826.531*	
23	*4810.535*	
24	*4842.529, 4562.419, 4376.354*	
25	**4810.536 (L-isoAsp[15]), 4796.523 (Ile12Nva)**	
Main Peak	4810.535 (Predicted: 4810.525, 2.1 PPM error)	
Green: observed in FA and TFA, **Blue**: identified impurity standard, Black: only observed with TFA		

Table 2. RP-HRMS Tirzepatide Monoisotopic Masses Observed (0.10% TFA).

In addition to the L-isoAsp[9] impurity, the results for the other impurity standards were also assessed (Table 1 & 2). The L-isoAsp[15] impurity was well separated and observed in both the FA (pre-main peak 27, Figure 2 and Table 1) and TFA separations (pre-main peak 16, Figure 3 and Table 2) with relative abundances of 0.09% to 0.11%. The Gln[19] and Gln[24] deamidation impurities eluted after the main peak in FA and TFA. While these impurities coeluted in FA, they were separated from one another with TFA. Of note, with TFA, the Gln[24] impurity is presumably coeluting with a variant that has a mass consistent with two sites of deamidation (post-main peak 2, Table 2 & Figure 3), this variant was not observed in the FA separation. The C-terminal deamidation impurity was tentatively assigned to a partially resolved trace-level peak shoulder in FA (post-main peak 3, Figure 2 and Table 1) but was not observed with TFA. The Ile12Nva substitution impurity was also observed as a partially resolved peak immediately preceding the main peak in both the FA (pre-main peak 33, Figure 2. Table 1) and

TFA (pre-main peak 25, Figure 4. Table 2). And finally, the D-Ser^{32} impurity was not adequately separated for MS identification in either the FA or TFA separations.

An example of the UV and MS sensitivity of these methods is illustrated by the detection and mass assignment of a trace level fragment with a predominant mass of 4486.261 which was identified as pre-main peak 4 in both the FA and TFA separations (Figures 2 and 3). The relative abundance was measured between 0.004% and 0.005% and the MS and A215 data quality is highlighted in the figures. The FA separation MS data quality outperforms that of the TFA separation while the TFA separation exhibits superior A215 data quality.

In total, these LC-HRMS results demonstrate some of the challenges involved in confirming the purity of these fatty-acid modified therapeutic peptides. While further optimization of these separations using this phenyl-hexyl RP column was not within the scope of this study, previously reported results indicate that improved resolution through the use of a 300 mm column along with extended gradients can provide greater separation of tirzepatide impurities when using 0.10% FA mobile phases.[1] The broad-range and steep gradient separations shown here suggest that this column may also be an effective option as a RP purity method to be paired with an orthogonal method (***e.g.*** HILIC or IEX).

In a concluding study, the separation performance of this charged surface phenyl-hexyl RP SPP column was compared to that of an alternative commercially available SPP phenyl-hexyl column with a charged surface. The principal specified differences between these columns are particle-size and pore-diameter. As noted, the column used for the previous studies has a 230 Å pore diameter and a 1.6 µm particle diameter. Comparatively, the alternative column is specified by the manufacturer as having a 90 Å pore diameter and a 2.7 µm particle diameter. The comparison presented (Figure 6) is for separation in 0.10% FA mobile phases. Both columns were 150 mm in length with internal diameters of 2.1 mm and were run using the same gradient. Following the FA evaluations, separations were also evaluated using 0.10% TFA as a mobile phase additive; however, these results are not presented here as the alternative column presented anomalous baseline behavior even after numerous blank gradients.

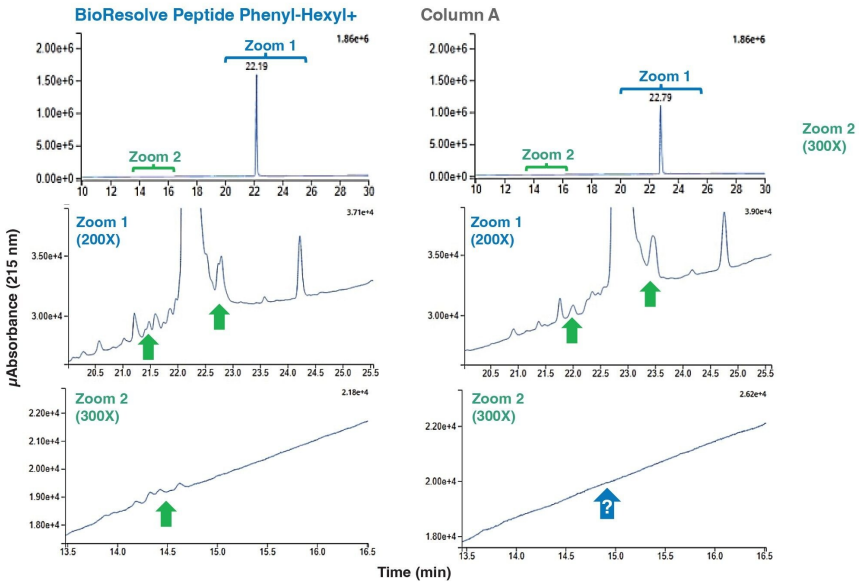

Figure 4. Comparison of A215 RP-LC profiles of a tirzepatide drug product are shown for a SPP Waters BioResolve Peptide Phenyl-Hexyl+ RP Column (SPP, 230 Å, 1.6 µm, 2.1 X150 mm) and an alternative SPP henyl-hexyl column (Column A, 90 Å, 2.7 µm, 2.1 X150 mm) with a positively charged surface. Both columns were tested with a 1% MeCN/min gradient with FA modifier (0.10% v/v).

Predictably, the Waters BioResolve Peptide Phenyl-Hexyl+ RP Column (MaxPeak Premier Technology, SPP, 1.6 µm, 230 Å) provided increased chromatographic detail and more sensitive low abundance impurity detection as compared to the alternative column. These observations are in line with the larger pore-diameter being more suitable for a nearly 5 kDa peptide and the smaller-particle size providing greater efficiency.[6]

Conclusion

The Waters BioResolve Peptide Phenyl-Hexyl+ RP Column (MaxPeak Premier Technology, SPP, 1.6 µm, 230 Å) provides a highly sensitive, selective approach for the RP-HRMS impurity profiling of tirzepatide that should also have applicability to other GLP-1a lipopeptides.

The charged-surface of this silica phenyl-hexyl SPP column provides effective separations, albeit with somewhat altered selectivities, in both FA and TFA containing mobile phases. Where improved MS sensitivity was observed with FA and improved optical sensitivity was observed with TFA, as would be predicted.

This column also outperformed an alternative SPP phenyl-hexyl column with charged 2.7 µm particle surfaces and a 90 Å pore diameter, a result that can be partially attributed to its larger 230 Å pore diameter and smaller 1.6 µm particle diameter.

While the presented RP methods using either FA or TFA as a mobile phase modifier can be further optimized with longer columns and extended gradients, the shorter analysis times of the presented LC and LCMS methods may be more amenable to be used alongside an orthogonal method or the implementation LCMS for improved impurity profile coverage to support both development and batch release.

References

1. Yang, H.; Shiner, S. Separation of a GLP-1 Receptor Agonist and Structurally Similar Impurities Using BioResolve™ Peptide Phenyl-Hexyl+ and C_{18}+ Columns. Application Brief 720009465 < https://www.waters.com/nextgen/global/library/application-notes/2026/separation-of-a-glp-1-receptor-agonist-and-structurally-similar-impurities-using-bioresolve-peptide-phenyl-hexyl-and-c18-columns.html> , Waters Corporation. June 2026.

2. Yoshida, Kenichi; ***et al***. Impurity profiling of synthetic cyclic peptides based on orthogonality between hydrophilic-interaction and reversed-phase liquid chromatography. Journal of Chromatography A 1745 (2025): 465748.

3. Han, D.; Ippoliti, S.; Birdsall, R. E.; Nyholm, K. Accelerating Method Development and Manufacturing of GLP-1 Analogs with LC-UV/MS. Application Note 720008800 < https://www.waters.com/nextgen/global/library/application-notes/2025/accelerating-method-development-and-manufacturing-of-glp-1-analogs-with-lc-uv-ms.html> , Waters Corporation, May 2025.

4. Goyon, A. (2026, June 6–16). Advanced chromatographic strategies for comprehensive characterization of therapeutic peptides [Keynote presentation]. 55th International Symposium on High Performance Liquid Phase Separations and Related Techniques (HPLC 2026), Indianapolis IN, USA, https://hplc2026-

symposium.org/program/keynote-speakers <https://hplc2026-symposium.org/program/keynote-speakers> .

5. Hanna, C. M.; Koza, S. M.; Shiner, S. Temperature Dependence on Reversed-Phase Separations of Fatty Acid Modified GLP-1 Receptor Agonists and Their Impurities. Application Note 720008590 < https://www.waters.com/nextgen/global/library/application-notes/2024/temperature-dependence-on-reversed-phase-separations-of-fatty-acid-modified-glp-1-receptor-agonists-and-their-impurities.html> , Waters Corporation. October 2024.

6. Koza, S. M.; Chambers, E. E. Selecting a Reversed-Phase Column for the Peptide Mapping Analysis of a Biotherapeutic Protein. Application Note 720005924 < https://www.waters.com/nextgen/global/library/application-notes/2017/reversed-phase-column-for-peptide-mapping-biotherapeutic-protein.html> . Waters Corporation, 2017.

Featured Products

ACQUITY Premier System < https://www.waters.com/nextgen/global/products/chromatography/chromatography-systems/acquity-premier-system.html>

Xevo G3 QTof <https://www.waters.com/nextgen/global/products/mass-spectrometry/mass-spectrometry-systems/xevo-g3-qtof.html>

BioResolve Columns <https://www.waters.com/nextgen/global/products/columns/bioresolve-columns.html>

waters_connect Software Solutions <https://www.waters.com/nextgen/global/products/informatics-and-software/waters_connect.html>

720009507, July 2026

© 2026 Waters Corporation. All Rights Reserved.
Condiciones de uso Aviso de privacidad de Waters Marcas comerciales Empleo Avisos legales y de privacidad Cookies Preferencias de cookies No vender mi información personal